

Low-pressure CO₂ sorption in ammonium-based poly(ionic liquid)s

Jianbin Tang^{a,b}, Huadong Tang^b, Weilin Sun^a, Maciej Radosz^b, Youqing Shen^{b,*}

^a Department of Polymer Science and Engineering, Zhejiang University, Hangzhou 310027, China

^b Soft Materials Laboratory, Department of Chemical and Petroleum Engineering, University of Wyoming, Laramie, WY 82071, USA

Received 19 September 2005; received in revised form 16 October 2005; accepted 17 October 2005

Available online 4 November 2005

Abstract

Ammonium-based ionic liquid monomers and their corresponding polymers [poly(ionic liquid)s] are synthesized and characterized for CO₂ sorption. The polymers have much higher CO₂ sorption capacities than the room-temperature ionic liquids and imidazolium-based poly(ionic liquid)s. For example, P[VBTMA][PF₆] with polystyrene backbone has a CO₂ sorption capacity of 10.67 mol%. The CO₂ sorption is selective over N₂ and O₂. The effects of cation, backbone, substituent, anion and crosslinking on CO₂ sorption are discussed. The sorption mechanism study indicates that CO₂ sorption by the poly(ionic liquid)s is a bulk and surface phenomenon.

© 2005 Elsevier Ltd. All rights reserved.

Keywords: Ionic liquids; Poly(ionic liquid)s; CO₂ sorption

1. Introduction

Ionic liquids, which are organic salts with low melting points, have remarkable CO₂-solubility [1–6]. They thus are explored as non-volatile and reversible CO₂ absorbents, and supported onto porous supports for developing supported liquid membranes (SLM) [7,8]. Recently, we found that the polymers made from imidazolium-based ionic liquid monomers, named poly(ionic liquid)s, had even higher CO₂ sorption capacity than room temperature ionic liquids with faster sorption/desorption rates [9]. The effects of the anion, cation and backbone on their CO₂ sorption capacity were found different from those of room temperature ionic liquids [10]. For example, cations in the poly(ionic liquid)s play a major role in their CO₂ sorption [10], while in ionic liquids, anions are the decisive parameter [3]. To further understand the effects of cations on the CO₂ sorption of poly(ionic liquid)s, we synthesized ammonium-based poly(ionic liquid)s and studied their CO₂ sorption. These polymers have further improved CO₂ sorption capacity compared with imidazolium-based poly(ionic liquid)s [11]. Similar to their corresponding fluoride salts, whose hydrated membrane showed high acid gas (CO₂, H₂S) permeability and high selectivity [12–17], these materials are promising as sorbent and membrane materials for CO₂ separation.

This paper reports the detailed syntheses and characterizations of the polymers, their CO₂ sorption isotherm, kinetics, and the effects of the polymer structures on the CO₂ sorption capacities.

2. Experimental

2.1. Materials

4-Vinylbenzyl chloride (90%), aqueous [2-(methacryloyloxy)ethyl]trimethyl ammonium chloride solution (75 wt%), (*p*-vinylbenzyl)trimethylammonium chloride (98%), triethylamine (99.5%), tributylamine (99.5%), *N,N,N',N'*-tetramethylethylenediamine (99%), lithium trifluoromethane sulfonimide (99.95%), potassium hexafluorophosphate (98%), sodium tetrafluoroborate (98%), 2, 6-di-*tert*-butyl-4-methyl phenol (98%) (DBMP), 2,2'-azobisisobutyronitrile (AIBN), *N,N*-dimethylformamide (99.8%) (DMF) and acetonitrile (99.5+%) were purchased from Aldrich. *o*-Benzoic sulphide sodium salt hydrate (97%) were purchased from Lancaster Synthesis Inc. All chemicals were used as received.

2.2. Synthesis of ionic liquid monomers

[2-(Methacryloyloxy)ethyl]trimethylammonium tetrafluoroborate ([MATMA] [BF₄]): aqueous [2-(methacryloyloxy)ethyl]trimethyl ammonium chloride solution (75 wt%) (30 ml, 0.12 mol) was added to a 250 ml flask. After the water was removed under vacuum, NaBF₄ (14.5 g, 0.132 mol) and

* Corresponding author. Tel.: +1 3077662501.

E-mail address: sheny@uwyo.edu (Y. Shen).

CH₃CN (150 ml) were added to the flask. The mixture was stirred over night. The salt dissolved gradually and a white precipitate formed. The precipitate was removed by filtration. The filtrate was concentrated, and then poured into ether. The precipitated white crystal was collected and dried in vacuum at room temperature (28 g, 90%).

(*p*-Vinylbenzyl)trimethylammonium tetrafluoroborate ([VBTMA][BF₄]), (*p*-vinylbenzyl)trimethylammonium hexafluorophosphate ([VBTMA][PF₆]), (*p*-vinylbenzyl)trimethylammonium *o*-benzoic sulphimide ([VBTMA][Sac]) (*p*-vinylbenzyl)trimethylammonium trifluoromethane sulfonamide (VBTMA)[Tf₂N]) were synthesized from *p*-vinylbenzyl trimethylammonium chloride as described above using NaBF₄, NaPF₆, *o*-Benzoic sulphimide sodium salt hydrate (NaSac) or lithium trifluoromethane sulfonamide (LiTf₂N) as ion exchange salts. The yields were 94.0, 90.0, 47.6, 41.9%, respectively.

[MATMA][BF₄]: ¹H NMR (DMSO-*d*₆, 400 MHz, ppm): δ 6.09 (d, 1H) 5.75(d, 1H) 4.53 (m, 2H) 3.70 (m, 2H) 3.14 (s, 9H) 1.91 (s, 3H). mp: 102.9–105.3 °C.

[VBTMA][BF₄]: ¹H NMR (DMSO-*d*₆, 400 MHz, ppm): δ 7.59 (d, 2H) 7.49(d, 2H) 6.78 (m, 1H) 5.94 (d, 1H) 5.36 (d, 1H) 4.47 (s, 2H) 3.00 (s, 9H). mp: 154.8–156.4 °C.

[VBTMA][PF₆]: ¹H NMR (DMSO-*d*₆, 400 MHz, ppm): δ 7.62 (d, 2H) 7.51(d, 2H) 6.81 (m, 1H) 5.96 (d, 1H) 5.39 (d, 1H) 4.50 (s, 2H) 3.02 (s, 9H). mp: 172.7–175.8 °C.

[VBTMA][Sac]: ¹H NMR (DMSO-*d*₆, 400 MHz, ppm): δ 7.58–7.69 (m, 6H) 7.52 (d, 2H) 6.81 (m, 1H) 5.96 (d, 1H) 5.38 (d, 1H) 4.53 (s, 2H) 3.04 (s, 9H).

[VBTMA][Tf₂N]: ¹H NMR (DMSO-*d*₆, 400 MHz, ppm): δ 7.61 (d, 2H) 7.51 (d, 2H) 6.81 (m, 1H) 5.94 (d, 1H) 5.37 (d, 1H) 4.50 (s, 2H) 3.02 (s, 9H) mp: 68.6 °C.

p-Vinylbenzyltriethylammonium tetrafluoroborate [VBTEA][BF₄] and *p*-vinyl benzyltributylammonium tetrafluoroborate [VBTBA][BF₄]: In 50 ml flask, 4-vinylbenzyl chloride (6.1 g, 0.04 mole) and triethylamine (4.2 g, 0.042 mol) was mixed, and heated at 50 °C under N₂ atmosphere for 2 day. The formed solid was collected and washed with diethyl ether. The resultant white solid (8.5 g, 0.033 mol) was mixed with NaBF₄ (3.8 g, 0.035 mole) in 50 mm acetonitrile, stirred at room temperature for 2 days. The salt precipitate was removed by filtration. The filtrate was concentrated and poured into 200 ml diethyl ether. The white crystal precipitate was collected by filtration, dried under vacuum. The total yield is 9.2 g (75%). [VBTBA][BF₄] was synthesized in similar procedure with a yield of 64%.

[VBTEA][BF₄]: ¹H NMR (DMSO-*d*₆, 400 MHz, ppm): δ 7.61 (d, 2H) 7.50 (d, 2H) 6.81 (m, 1H) 5.96 (d, 1H) 5.39 (d, 1H) 4.46 (s, 2H) 3.16 (m, 6H) 1.31 (m, 9H). mp: 117.5–120.2 °C.

[VBTBA][BF₄]: ¹H NMR (DMSO-*d*₆, 400 MHz, ppm): δ 7.63 (d, 2H) 7.46(d, 2H) 6.80 (m, 1H) 5.97 (d, 1H) 5.39 (d, 1H) 4.51 (s, 2H) 3.11 (m, 6H) 1.74 (m, 6H) 1.32 (m, 6H) 0.96 (m, 9H). mp: 105.8–107.4 °C.

1,2-Bis(*p*-vinylbenzyl)dimethylammonium ethane [BVDEA][BF₄]: *N,N,N',N'*-Tetramethylethylenediamine (5.8 g, 0.05 mol), 4-vinylbenzyl chloride (16.0 g, 0.105 mol) and 0.1 g DBMP were mixed in 50 ml DMF. The resulting solution was heated at 50 °C for 2 days. The solution was

poured into 400 ml of diethyl ether to precipitate out the product. After filtration and drying under vacuum, 15.8 g of white crystal product was obtained. The product was reacted with NaBF₄ (4.3 g, 0.04 mol) in 50 ml of dried acetonitrile for 2 days. After the reaction, the insoluble chloride salt was removed by filtration. The product was precipitated by ether, collected by filtration and dried under vacuum. The overall yield is 16.7 g (63.7%) ¹H NMR (DMSO-*d*₆, 400 MHz, ppm): δ 7.66 (d, 4H) 7.59(d, 4H) 6.83 (m, 2H) 5.99 (d, 2H) 5.41 (d, 2H) 4.60 (s, 4H) 3.94 (s, 4H) 3.07(s, 12H).

Dodecyltriethyl ammonium trifluoromethane sulfonamide ([DTEA][Tf₂N]): 1-bromododecane (4.2 ml, 0.0175 mol) and excess triethylamine (8 ml) were mixed and heated at 60 °C for 5 days. The formed white precipitate and was collected by filtration. After drying under vacuum, the precipitate (4.2 g, 0.012 mol) was mixed with lithium trifluoromethane sulfonamide (3.8 g, 0.013 mol) in 25 ml of dry acetone. This mixture was stirred for 2 days. The salt precipitate was removed by filtration. The filtrate was concentrated, and then poured into diethyl ether. A transparent viscous liquid was collected by centrifuge, and dried under vacuum. The overall yield is 4.8 g (51%). ¹H NMR (CDCl₃, 400 MHz, ppm): 3.26 (m, 6H), 3.07 (m, 2H), 1.62 (m, 2H) 1.15–1.4 (m, 27H), 0.88 (m, 3H) mp: 2 °C.

2.3. Synthesis of poly(ionic liquid)s

The polymers were synthesized via free radical polymerization using AIBN as initiator. A typical example is as following: [VBTMA][BF₄] (3 g), AIBN (30 mg) and DMF (3 ml) were charged into a reaction tube. The tube was tightly sealed, and degassed. It was immersed in an oil bath at 60 °C for 6 h. The solution was poured into methanol to precipitate out the polymer. The polymer was dried under vacuum at 100 °C. The yield was 2.85 g (95%).

P[MATMA][BF₄]: ¹H NMR (DMSO-*d*₆, 400 MHz, ppm): 4.33 (br, 2H), 3.67 (br, 2H), 3.16 (s 9H), 2.2–0.2 (m, 14H). Anal. Calcd for C₉H₁₈NO₂BF₄: C, 41.7 H, 7.0; N, 5.4. Found: C, 40.45; H, 6.80; N, 5.12.

P[VBTMA][BF₄]: ¹H NMR (DMSO-*d*₆, 400 MHz, ppm) 7.08 (br, 2H), 6.50 (br, 2H), 4.30 (br, 2H) 2.92 (br, 9H), 1.81 (br, 1H), 1.48 (br, 2H). Anal. Calcd for C₁₂H₁₈NBF₄: C, 54.8; H, 6.8; N, 5.3. Found: C, 55.21; H, 6.1; N, 5.4.

P[VBTMA][SAC]: ¹H NMR (DMSO-*d*₆, 400 MHz, ppm) 7.50–8.20 (m, 4H), 6.90–7.50 (br, 2H), 6.20–6.9 (br, 2H) 4.53 (br, 2H), 2.92 (s, 9H), 0.8–2.3 (br, 3H). Anal. Calcd for C₁₉H₂₂N₂O₃S: C, 63.7; H, 6.14; N, 7.8. Found: C, 62.27; H, 6.12; N, 7.66.

P[VBTMA][Tf₂N]: ¹H NMR (DMSO-*d*₆, 400 MHz, ppm) 7.01 (br, 2H), 6.49 (br, 2H), 4.28 (br, 2H) 2.85 (br, 9H), 1.99 (br, 1H), 1.44 (br, 2H). Anal. Calcd for C₁₄H₁₈N₂O₄S₂F₆: C, 36.84; H, 3.95; N, 6.14. Found: C, 36.59; H, 3.95; N, 6.01.

P[VBTMA][PF₆]: ¹H NMR (DMSO-*d*₆, 400 MHz, ppm) 7.16 (br, 2H), 6.58 (br, 2H), 4.24 (br, 2H) 2.86 (br, 9H), 2.01 (br, 1H), 1.43 (br, 2H) Anal. Calcd for C₁₅H₁₈NBF₄: C, 44.86; H, 5.60; N, 4.36. Found: C, 43.97; H, 5.63; N, 4.26.

P[VBTEA][BF₄]: ¹H NMR (DMSO-*d*₆, 400 MHz, ppm) 7.13 (br, 2H), 6.54 (br, 2H), 4.27 (br, 2H) 3.05 (br, 6H),

2.30–0.70 (m, 12H) Anal. Calcd for $C_{15}H_{24}NBF_4$: C, 59.0; H, 7.87; N, 4.59. Found: C, 58.17; H, 8.10; N, 4.28.

P[VBTTBA][BF₄]: ¹H NMR (DMSO-*d*₆, 400 MHz, ppm) 7.08 (br, 2H), 6.54 (br, 2H), 4.40 (br, 2H) 3.02 (br, 6H), 2.30–0.20 (m, 24H). Anal. Calcd for $C_{21}H_{36}NBF_4$: C, 64.8; H, 9.26; N, 3.6. Found: C, 65.10; H, 9.40; N, 3.49.

2.4. Measurements

¹H NMR spectra were measured on a Bruker Advance DRX-400 spectrometer using deuterated dimethylsulfoxide (DMSO-*d*₆) as solvent. The elemental analysis was done by Midwest Microlab LLC (US). The X-ray diffraction (XRD) analysis was recorded on a SCINTAG XDS2000 automated powder diffraction system operating in normal transmission mode with Ni-filtered Cu K α radiation. Differential scanning calorimetric (DSC) experiments were performed on a TA Instruments DSC Q900 differential scanning calorimeter. The samples were heated to 200 °C and then cooled to room temperature. The glass transition temperatures (*T*_gs) were calculated in the second scanning at a heating rate of 20 °C min⁻¹. Scanning electron microscope was operated on a model Philips 505. The BET surface areas of the powders were determined by nitrogen adsorption (Tristar 3000, Micromeritics Instruments Corp.).

2.5. CO₂ sorption and desorption

The CO₂ sorption of the poly(ionic liquid)s was measured using a CAHN 1000 Electrobalance (Scheme 1). The sample pan and the counterweight of the balance were configured symmetrically to minimize buoyancy effects. The microbalance has 100 g capacity and 1.0 μ g sensitivity and is suitable for study of adsorption and diffusion of gases on/in solid or liquid materials. CO₂ gas (99.995%) was dried by passing two drying columns (length \times diameter: 15 in. \times 2 in.) packed with P₂O₅. The fine powder of the ionic liquid polymer was dried and degassed at 70 °C under vacuum for 12 h to remove moisture or other volatile contaminants. It was further dried in the balance by evacuating the chamber at high vacuum until its weight reached constant for at least 30 min. CO₂ was

introduced into the chamber and the sample weight was recorded until it did not change significantly in 30 min. The buoyancy effects in these measurements were corrected according to literature [17]. The sorption capacities were presented as mol% of the monomer units, which were calculated by '(N - CO₂/N - monomer units) \times 100%'.

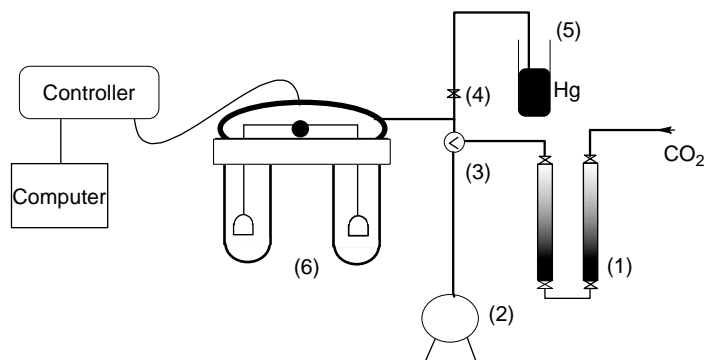
3. Results and discussion

3.1. Synthesis and characterization of ionic-liquid monomers

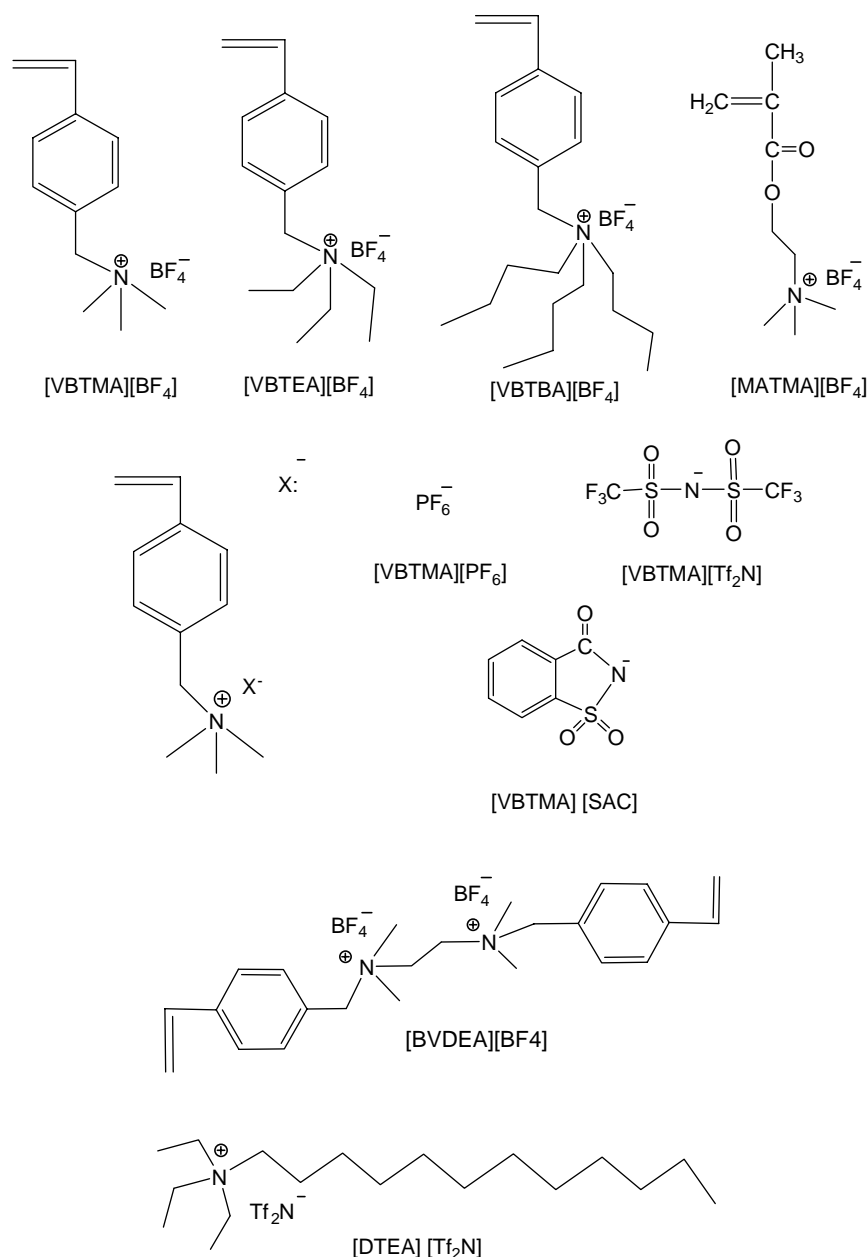
The structures of ionic liquid monomers are shown in Scheme 2. They were synthesized from ammonium halide precursors are soluble in water and DMF, but insoluble in acetone and acetonitrile, while their corresponding ionic liquid monomers with BF₄ anion are not only soluble in water and DMF, but also in acetone and acetonitrile. At room temperature, [MATMA][BF₄], [VBTTMA][BF₄], [VBTTMA][PF₆], [VBTTMA][Tf₂N], [VBTEA][BF₄], [VBTTBA][BF₄] are crystal solids. [VBTTMA][Sac] is a viscous liquid. All these monomers are soluble in highly polar solvents such as DMF, DMSO, acetonitrile and acetone, insoluble in low polar and non-polar solvents such as diethyl ether and hexane. They also have different water solubility: [VBTTMA][BF₄], [MATMA][BF₄], [VBTEA][BF₄], [VBTTMA][Sac] are soluble in water, while [VBTTMA][PF₆], [VBTTMA][Tf₂N] and [VBTTBA][BF₄] are insoluble in water.

3.2. Syntheses of poly(ionic liquid)s

Poly(ionic liquid)s were prepared from the ionic liquid monomers by free radical polymerization using AIBN as an initiator. DMF was used as solvent because all poly(ionic liquid)s are soluble in it. Poly(ionic liquid)s were precipitated in methanol or dichloromethane to remove unreacted monomers. DMF residue in polymers was removed by drying at 100 °C under vacuum. Poly(ionic liquid)s with different substituents and anions have different water-solubility. For instance, P[VBTTMA][BF₄], P[MATMA][BF₄], P[VBTEA][BF₄] are soluble in H₂O. P[VBTTMA][Tf₂N] and P[VBTTMA]



Scheme 1. Schematic diagram of gas sorption/desorption apparatus. Dryer (P₂O₅) columns (1); vacuum pump (2); 3-way valve (3), 2-way valve (4), mercury reservoir (5), Cahn 1000 electrobalance (6).



Scheme 2. The structures of the monomers and the room temperature ionic liquid [DTEA][Tf₂N].

[Sac] are partially soluble in H₂O. P[VBTBA][BF₄] and P[VBTMA][PF₆] are insoluble in H₂O. All poly(ionic liquids) are soluble in highly polar solvent such as DMF, DMSO, acetonitrile (except P[VBTMA][Sac]), insoluble in low polar and non-polar solvent such as diethyl ether and hexanes. ¹H NMR spectra and element analyses indicated that pure poly(ionic liquid)s were obtained.

3.3. Thermal properties of poly(ionic liquid)s

The DSC curves of poly(ionic liquid)s are shown in Fig. 1. The anions strongly affected the glass transition temperatures of the polymers (Fig. 1(1)). The *T_g*s of the polymers with poly(*p*-vinylbenzyltrimethylammonium)(P[VBTMA]) backbone but different anions are as following: P[VBTMA][Sac]

(65 °C) < P[VBTMA][Tf₂N] (74 °C) < P[VBTMA][BF₄] (235 °C) < P[VBTMA][PF₆] (255 °C). The organic Tf₂N⁻ and Sac⁻ anions can substantially reduce the *T_g*s of the polymers. This is caused by the plasticization of the anions. Fig. 1(2) shows the DSC curves of poly(ionic liquid)s with the same anion (BF₄⁻) but with different cations. Their *T_g*s are as follows: P[VBTBA][BF₄] (135 °C) < P[VBTEA][BF₄] (185 °C) < P[MATMA][BF₄] (216 °C) < P[VBTMA][BF₄] (235 °C). The *T_g* of the polymer decreases with increasing the length of substituent alkyl chain on the ammonium cation from methyl to butyl. P[VBTMA][BF₄] with polystyrene backbone have higher *T_g* than P[MATMA][BF₄] with polymethylmethacrylate. Therefore, the anion, substituent on the cation and backbone of poly(ionic liquid)s affect their glass transition temperatures.

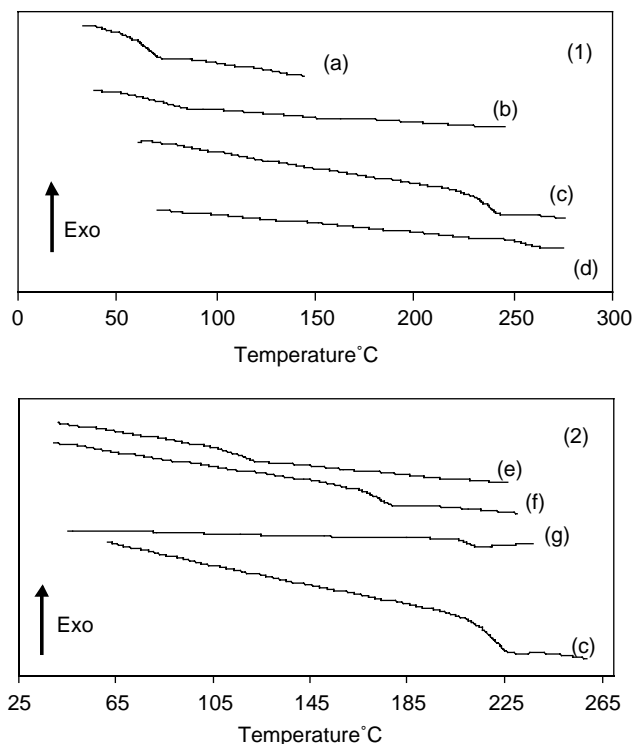


Fig. 1. DSC curves of the poly(ionic liquids) with different anions (1) and backbones (2). P[VBVTMA][Sac](a), P[VBVTMA][Tf₂N](b), P[VBVTMA][BF₄](c), [VBVTMA][PF₆](d), P[VBVTBA][BF₄](e), P[VBTEA][BF₄](f), P[MATMA][BF₄](g).

The X-ray diffraction spectra of P[VBVTMA][BF₄] and P[MATMA][BF₄] are shown in Fig. 2. There was no crystalline peak in the XRD patterns in the polymers, which indicated the polymers are amorphous.

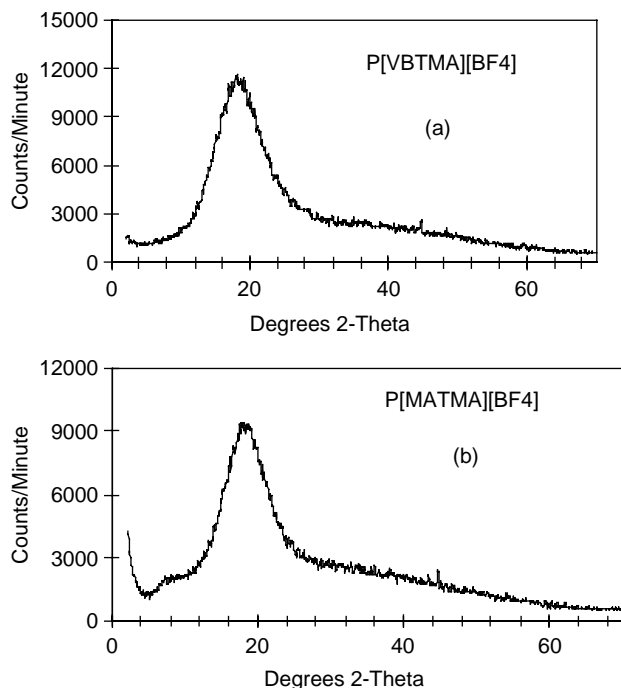


Fig. 2. XRD patterns of poly(ionic liquids). (a) P[VBVTMA][BF₄]; (b) P[MATMA][BF₄].

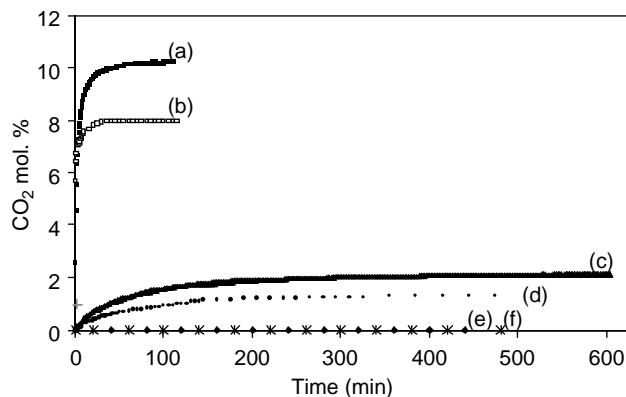


Fig. 3. The CO₂ sorption kinetics of the poly(ionic liquids), their corresponding monomers, and a room temperature ionic liquid (592.3 mmHg CO₂, 22 °C). P[VBVTMA][BF₄](a), P[MATMA][BF₄](b), [DTEA][BF₄](c), [bmim][BF₄](d), [VBVTMA][BF₄](e), [MATMA][BF₄](f).

3.4. CO₂ sorption kinetics of the poly(ionic liquids)

CO₂ has remarkable solubility in imidazolium-based ionic liquids because of its interactions with the anions and cations of ionic liquids [3]. The CO₂ sorption of poly(ionic liquids) and their corresponding monomers was tested and is shown in Fig. 3. The CO₂ solubility of [bmim][BF₄] was tested first and found consistent with that reported in literature [3], which validated the setup of the apparatus.

At equilibrium, P[VBVTMA][BF₄] and P[MATMA][BF₄] took up 10.22, and 7.99 mol% of CO₂, respectively, in terms of their monomer units. These are about four to five times of the capacities of imidazolium-based poly(ionic liquids) [9,10]. Their monomers, [VBVTMA][BF₄] and [MATMA][BF₄], had no measurable sorption of CO₂ because of their crystalline structures. Furthermore, room temperature ionic liquids, imidazolium-based [bmim][BF₄] and ammonium-based [DTEA][Tf₂N] only absorbed 1.34 and 2.09 mol% of CO₂ under the same conditions. Similar to the imidazolium-based poly(ionic liquids), the CO₂ sorptions of these poly(ionic liquids) were also fast. It took only several minutes to reach their 90% capacity and less than 60 min to reach the equilibrium.

3.5. Isotherms of CO₂ sorption of poly(ionic liquids)

The sorption isotherms of P[VBVTMA][BF₄] and P[MATMA][BF₄] at different CO₂ pressures and 22 °C are shown in Fig. 4. The CO₂ mole fraction in the polymers increased with the increase of CO₂ pressure. Henry's constant is defined as:

$$H_i = \lim_{x_i \rightarrow 0} \frac{P_i}{x_i}$$

where H_i is the Henry's constant, x_i is the mole fraction of gas sorbed in the polymer in term of monomeric unit, and P_i is the CO₂ pressure. Since the x_i vs. P_i plots were not linear in the entire pressure range, the Henry's constants were calculated by fitting the data and extrapolating the slope to the zero CO₂

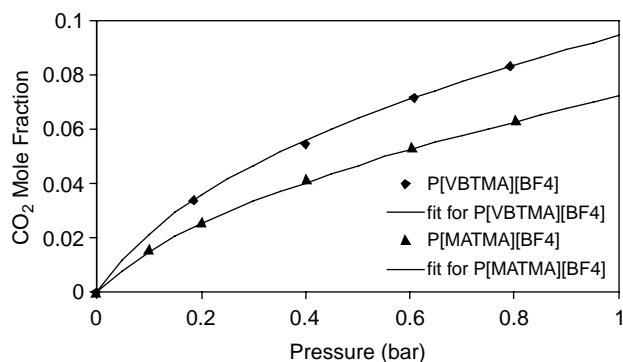


Fig. 4. Isothermal sorption of P[VBTMA][BF₄] and P[MATMA][BF₄] at different CO₂ pressures (22 °C).

partial pressure [6]. The calculated Henry's constant was 3.7 bar (22 °C) for P[VBTMA][BF₄] and 5.4 bar (22 °C) for P[MATMA][BF₄], which are much lower than that of imidazolium-based poly(ionic liquid)s. (26.0 bar for P[VBBI][BF₄] and 37.7 bar for P[MABI][BF₄] at 22 °C) [10].

3.6. The sorption selectivity of poly(ionic liquid)s

The CO₂ sorption of the polymers is selective, as shown in Fig. 5. There was no measurable weight increase when the polymers were exposed to N₂ or O₂ under the same conditions, indicative of that poly(ionic liquid)s selectively take up CO₂.

3.7. Repeated CO₂ sorption and desorption

Four cycles of CO₂ sorption and desorption of P[VBTMA][BF₄] and P[MATMA][BF₄] were tested by filling the chambers with CO₂ and then vacuuming (Fig. 6). The sorption and desorption of P[VBTMA][BF₄] and P[MATMA][BF₄] were all fast. It took only about 60 min to take up CO₂ and to have a complete desorption of CO₂. The desorption was complete, suggesting that the sorption/desorption was reversible. No change in sorption/desorption kinetics and sorption capacity was observed after four cycles.

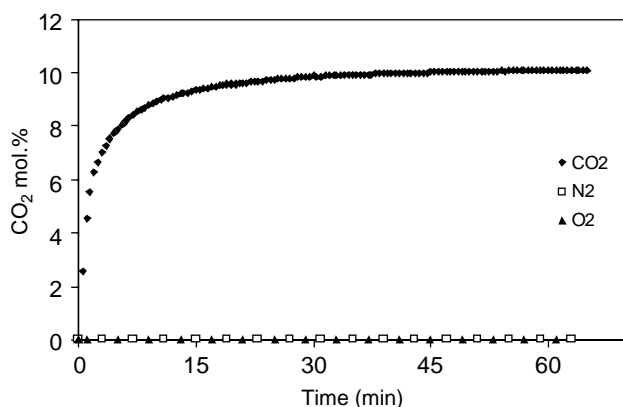


Fig. 5. Gas (CO₂, O₂, N₂) sorption of P[VBTMA][BF₄] as a function of time at 592.3 mmHg, 22 °C.

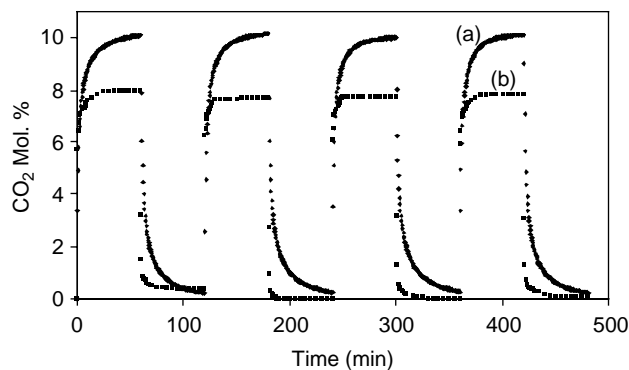


Fig. 6. Cycles of CO₂ sorption (592.3 mmHg CO₂, 22 °C) and desorption by vacuuming of P[VBTMA][BF₄] (a) and P[MATMA][BF₄] (b).

3.8. The effect of poly(ionic liquid)s structure on CO₂ sorption

The CO₂ sorption of poly(ionic liquid)s with different backbones, cations, and anions was compared to study the structure effect on CO₂ sorption. The CO₂ sorption kinetics of poly(ionic liquid)s with different backbones are shown in Fig. 7. At equilibrium, P[VBTMA][BF₄] took up 10.22 mol%, and P[MATMA][BF₄] sorbed 7.99 mol%, respectively, in terms of their monomer units at 592.3 mmHg of CO₂ and 22 °C. With the same ammonium cation and BF₄⁻ anion,

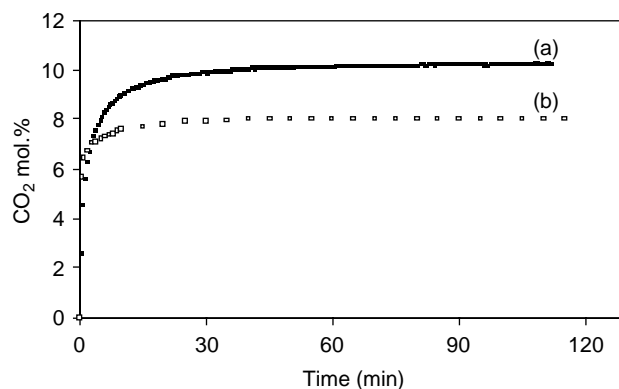


Fig. 7. CO₂ sorption in poly(ionic liquid)s with different backbones (592.3 mmHg CO₂, 22 °C). P[VBTMA][BF₄] (a), P[MATMA][BF₄] (b).

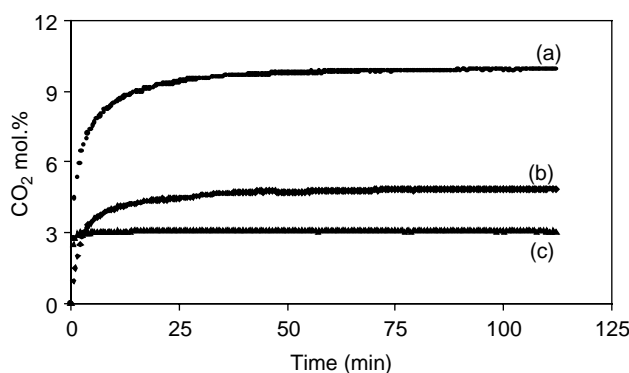


Fig. 8. CO₂ sorption in poly(ionic liquid)s with different substituents (592.3 mmHg CO₂, 22 °C). P[VBTMA][BF₄] (a), P[VBTEA][BF₄] (b), P[VBTEA][BF₄] (c).

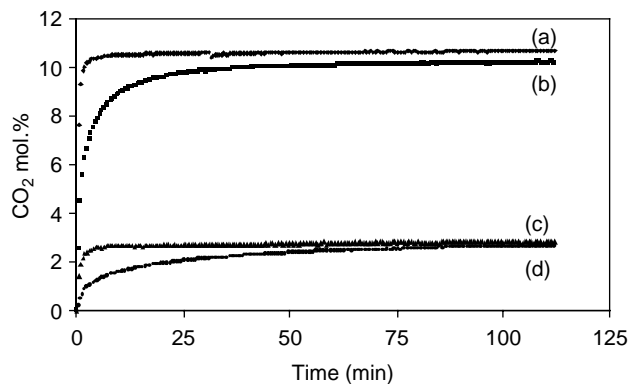


Fig. 9. CO₂ sorption in poly(ionic liquid)s with different anions (592.3 mmHg CO₂, 22 °C). P[VBTMA][PF₆] (a), P[VBTMA][BF₄] (b), P[VBTMA][Tf₂N] (c), P[VBTMA][Sac] (d).

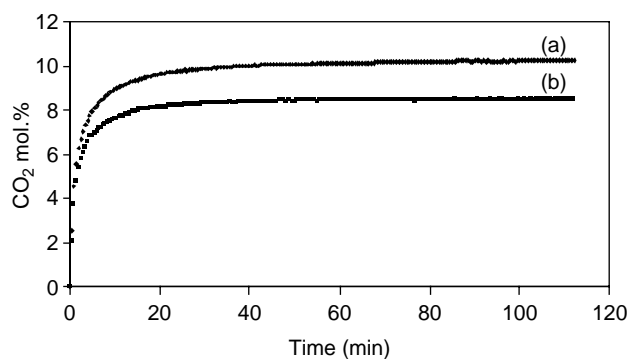


Fig. 10. The effect of crosslinking on CO₂ sorption (592.3 mmHg CO₂, 22 °C). Non-crosslinked P[VBTMA][BF₄] (a), 5% crosslinked P[VBTMA][BF₄] (b).

the polymer with polystyrene backbone had a higher CO₂ sorption capacity than that with polymethylmethacrylate.

The effect of substituent on the ammonium cation on the CO₂ sorption is shown in Fig. 8. Their capacities of CO₂ sorption are as follows: P[VBTMA][BF₄] (10.2 mol%) > P[VBTEA][BF₄] (4.85 mol%) > P[VBTBA][BF₄] (3.1 mol%). Obviously, the CO₂ sorption capacity decreases with increasing the chain length of the substituent, which indicates that a large substituent on the ammonium cation blocks CO₂ sorption.

The effect of the anions on the CO₂ sorption capacity of the poly(ionic liquid)s is shown in Fig. 9. The CO₂ sorption

capacity of the P[VBTMA]-based polymers depends on the anion types. It was 10.66 mol% for P[VBTMA][PF₆], 10.22 mol% for P[VBTMA][BF₄], 2.85 mol% for P[VBTMA][Tf₂N] and 2.67 mol% for P[VBTMA][Sac], respectively. This trend is the same as imidazolium-based poly(ionic liquid)s with different anions but totally different from that of small molecular ionic liquids [3]. The poly(ionic liquid)s with Tf₂N⁻ anions had a sorption capacity much lower than those with PF₆⁻ and BF₄⁻ anions (P[VBTMA][PF₆], P[VBTMA][BF₄]), and similar to the capacity of the poly(ionic liquid) with non-fluorine anions (P[VBTMA][Sac]). These results indicate that for poly(ionic liquid)s fluorine-atoms are not a decisive factor for CO₂ sorption and polymers with inorganic anions have higher capacity.

The effect of crosslinking on CO₂ sorption in P[VBTMA][BF₄] are shown in Fig. 10. P[VBTMA][BF₄] crosslinked with 5% [BVDEA][BF₄] had a *T_g* at 220 °C, its CO₂ sorption capacity decreased by 20%, which might be due to the decreased void volume of polymer upon crosslinking.

3.9. Sorption mechanism

The BET surface area of P[VBTMA][BF₄] and P[MATMA][BF₄] were measured by nitrogen adsorption, and their morphology was examined by SEM. The specific surface area of the particles measured by BET were 0.46 m²/g for P[VBTMA][BF₄], 20.5 m²/g for P[MATMA][BF₄]. The SEM (Figs. 11 and 12) indicated that P[VBTMA][BF₄] particles were non-porous, while P[MATMA][BF₄] particles were porous. This result is consistent with the BET surface area measurement. The calculated CO₂-adsorption assuming a monolayer of CO₂ on the surface were only 0.02 wt% for P[VBTMA][BF₄] and 0.89 wt% for P[MATMA][BF₄], much less than the measured CO₂ sorption capacities. Furthermore, P[VBTMA][BF₄] had much lower surface area but higher CO₂ sorption capacity than P[MATMA][BF₄]. P[MATMA][BF₄] with porous structure had faster CO₂ sorption and desorption rate than P[VBTMA][BF₄] with non-porous structure (Fig. 6). Therefore, the CO₂ sorption capacity mainly depends on the chemical structure of poly(ionic liquid)s, while the rate of CO₂ sorption affected by the surface area of the polymers.

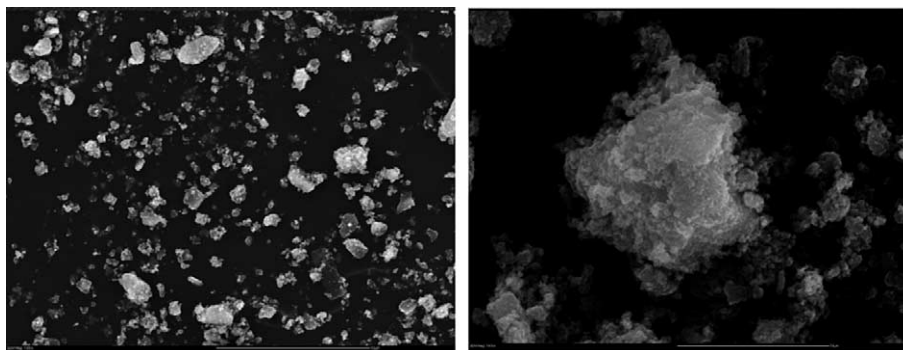


Fig. 11. SEMs of P[MATMA][BF₄].

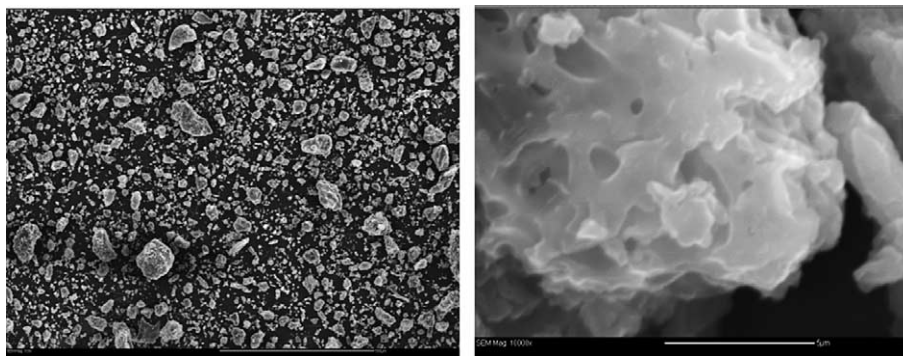


Fig. 12. SEMs of P[VTMA][BF₄].

We propose that the CO₂ sorption of the polymer particles involves absorption (the bulk) and adsorption (the surface).

4. Conclusion

Ammonium-based ionic liquid monomers and their corresponding polymers [poly(ionic liquids)] were synthesized and characterized for CO₂ sorption. The polymers have higher CO₂ sorption capacities than the room-temperature ionic liquids and imidazolium-based poly(ionic liquid). The measured Henry's constants for CO₂ in P[VTMA][BF₄] and P[MTMA][BF₄] are 3.7 and 5.4 bar, respectively, lower than imidazolium-based poly(ionic liquid). The CO₂ sorption is selective over N₂ and O₂. P[VTMA][PF₆] having polystyrene backbone, inorganic anion and small substituent on cation has the highest CO₂ sorption capacity of 10.66 mol%. The CO₂ sorption capacity of P[VTMA][BF₄] decreases 20% after 5% crosslinked. The CO₂ sorption is a bulk and surface phenomenon.

Acknowledgements

We thank the State of Wyoming (EORI) and the University of Wyoming for financial support.

References

- [1] Blanchard LA, Hancu D, Beckman EJ, Brennecke JF. *Nature* 1999;399:28–9.
- [2] Blanchard LA, Gu ZY, Brennecke JF. *J Phys Chem B* 2001;105:2437–44.
- [3] Cadena C, Anthony JL, Shah JK, Morrow TI, Brennecke JF, Maginn E. *J Am Chem Soc* 2004;126:5300–8.
- [4] Scovazzo P, Camper D, Kieft J, Poshusta J, Koval C, Noble RD. *Ind Eng Chem Res* 2004;43:6855–60.
- [5] Camper D, Scovazzo P, Koval C, Noble RD. *Ind Eng Chem Res* 2004;43:3049–54.
- [6] Anthony JL, Maginn EJ, Brennecke JF. *J Phys Chem B* 2001;106:7315–20.
- [7] Bates ED, Mayton RD, Ntai I. *J Am Chem Soc* 2002;124:926.
- [8] Fortunato R, Afonso CAM, Reis MAM, Crespo JG. *J Membr Sci* 2004;242:197–209.
- [9] Tang JB, Sun WL, Tang HD, Radosz M, Shen Y. *Macromolecules* 2005;38:2037–9.
- [10] Tang JB, Sun WL, Tang HD, Radosz M, Shen Y. *J Polym Sci, Part A: Polym Chem*. 2005;43:5477–89.
- [11] Tang JB, Sun WL, Tang HD, Plancher H, Radosz M, Shen Y. *Chem Commun* 2005;3325–7.
- [12] Quinn R, Laciak DV. *J Membr Sci* 1997;131:61–9.
- [13] Quinn R, Laciak DV, Pez GP. *J Membr Sci* 1997;131:49–60.
- [14] Quinn R, Laciak DV, Appleby JB, Pez GP. US Patent 5336298; 1994.
- [15] Quinn R, Laciak DV, Pez GP. US Patent 6315968; 2001.
- [16] Quinn R. *J Membr Sci* 1998;139:97–102.
- [17] Macedonia MD, Moore DD, Maginn EJ. *Langmuir* 2000;16:3823–34.